Contents lists available at www.innovativejournal.in
INNOVATIVE JOURNAL OF MEDICAL AND HEALTH SCIENCE
Available online at
http://www.innovativejournal.in/index.php/ijmhs

ONLINE ISSN:2277-4939
PRINT ISSN:2589-9341

Evaluation of MRI based diagnostic algorithm for intra-axial brain masses: A single centre experience

Virender Malik, Debraj Sen, Dr. Abha Kumari*

Department of Radiodiagnosis, Military Hospital Jodhpur, India, Jodhpur â€“342006

Correspondence Author: **Dr. Abha Kumari**

Abstract:-Background and Purpose: *Preoperative evaluation and differentiation of intra-axial brain masses is essential for therapy and prognosis. The integrated Magnetic Resonance Imaging (MRI) techniques such as Diffusion Weighted Imaging (DWI), Magnetic Resonance Spectroscopy (MRS) and Dynamic Susceptibility Contrast (DSC) MRI allow insights into tumour anatomy and physiology. Our study was designed to find the sensitivity, specific and accuracy of a diagnostic algorithm comprising of these techniques.*

Materials and Methods: *Thirty consecutive immunocompetent patients with treatment naïve intra-axial brain masses underwent MRI from July 2016 to July 2017. Conventional and DWI, MRS and MR perfusion scans were performed using 1.5 T MR imaging system. The following cut-off values (ADC ≤1.1 /100mm^2, intralesional Cho/NAA > 2.2, perilesional Cho/NAA >1 and rCBV >1.75) were applied to the diagnostic strategy algorithm. Histopathological analysis served as the gold standard. Sensitivity, specificity, negative predictive value (NPV), positive predictive value (PPV) and accuracy were obtained.*

Results: *Twenty one of 30 cases were correctly classified using the diagnostic algorithm. One case of primary central nervous system lymphoma (PCNSL) was misdiagnosed as metastasis, 2 cases of high-grade neoplasm (HGN) as brain abscesses, 1 case of HGN as metastasis, 1 case of HGN as low-grade neoplasm (LGN), 1 case of LGN as HGN, 1 case of LGN as abscess / tumefactive demyelinating lesion (TDL), 1 case of brain abscess as HGN, and 1 case of metastasis (breast carcinoma) as HGN.*

Conclusion: *Diagnosing intra-axial brain masses using a combination of advanced imaging techniques (MRS, MR perfusion and ADC) is fairly accurate.*

Keywords:-*Diagnostic algorithm; Intra-axial brain masses; Magnetic Resonance Imaging (MRI); Diffusion-weighted imaging (DWI); MR spectroscopy (MRS); MR perfusion*

Introduction:

The preoperative evaluation and differentiation of intra-axial brain masses is essential for determining the best possible neurosurgical strategy and patient prognostication. The integration of information obtained from advanced magnetic resonance imaging (MRI) techniques plays an important diagnostic and prognostic role in intra-axial brain masses. These techniques not only provide anatomical details but also provide insight into the underlying physiological processes and aid in arriving at a specific diagnosis.

The differentiation of common intra-axial masses using a diagnostic algorithm, comprising several parameters and a few cut-off values has been Advocated by Al-Okaili RN *et al*[1]. Our study comprising of 30 patients is designed to find the sensitivity, specific and accuracy of this diagnostic algorithm

Materials and methods:

Patient Selection: The study was carried out at a tertiary oncology centre after obtaining approval of the institutional review board and informed

Consent from all patients. Eligible patients fulfilling the inclusion criteria of age more than 18 years, immunocompetent status, presence of treatment-naïve intra-axial brain mass, absence of imaging features suggestive of benign disease process (like calcified granuloma) on conventional MRI at our institute from July 2016 to July 2017 were included. A total of 30 consecutive patients

fulfilling the inclusion criteria were included in the study.

MR imaging, post-processing and analysis: Images were acquired using a 1.5 T MR imaging system (Siemens Magnetom Symphony) with a 12-channel head-matrix coil. Conventional MR imaging included axial T2 weighted fast spin echo (FSE) sequence (Slice thickness: 5mm, TR/TE: 4210/99, FOV: 230 x 173 mm), FLAIR axial sequence (Slice thickness: 5mm, TR/TE/TI: 8200/114/2500 ms respectively, FOV: 230 x 173 mm), 3DT1 sequence (TR/TE: 11/5.2 ms, FOV: 224 x 256 mm). Matrix size was 384 x 512 in T2WI and 308 x 512 for FLAIR sequence. The echo-planar imaging (EPI) diffusion-weighted imaging (DWI) sequence was performed using sequential application of diffusion sensitizing gradients (b values of 0, 500 and 1000 s/mm^2 in three orthogonal directions). Post-processing of apparent diffusion coefficient (ADC) maps was performed. The lowest ADC value (expressed in mm^2/s) from 5 regions of interest of enhancing and non-enhancing parts of a lesion was recorded. Subsequently perfusion imaging was done using T2* weighted EPI sequence. After the second dynamic acquisition, a standard dose (0.1 mmol/kg body weight) of Gadopentetate dimeglumine was injected as a bolus through a pneumatically driven injection pump at a rate of 5 mL/s. Contrast injection was followed by 20 ml of saline bolus. After completion of the Dynamic Susceptibility Contrast (DSC)-MR sequence, standard post contrast 3D T1 data was acquired. Single voxel Magnetic Resonance Spectroscopy (MRS) was obtained from the enhancing portion, immediately outside of the enhancing portion and from the corresponding contralateral white matter (WM). The Cho/NAA ratio was then measured from these areas. Post-processing of perfusion images was obtained using software developed at the institute – 'Promatheus'. The recorded cerebral blood volume (CBV) value from the lesion area was normalized to contralateral normal-appearing white matter (NAWM) and relative CBV (rCBV) obtained. The maximum rCBV value was chosen from among the 3 recorded values. Subsequently the conventional and advanced MRI (DWI, MRS and MR perfusion) findings were integrated and applied to the diagnostic algorithm. Histopathological examination (HPE) was done for all cases and served as the gold standard for the study. Statistical analysis was performed using the Statistical Package for the Social Sciences Statistics, Version 20.0 (IBM, Armonk, New York). P values < 0.05 were considered significant.

Results:

Our study comprising 30 patients (17 males, 13 females), included HPE diagnosis of high grade neoplasm (HGN, n=14), low grade neoplasm (LGN, n=6), metastases (n=5), primary central nervous system lymphoma (PCNSL) (n=2) and brain abscess (n=3). Applying advanced imaging cut-off values to the diagnostic algorithm, we correctly classified 21 of 30 cases (Fig 1 and Table 1).

Of the nine (9) inaccurately diagnosed cases, eight (8) were enhancing lesions and one (1) a non-enhancing lesion. Out of the 30 lesions, 23 (cases) showed enhancement; 11 out of 14 HGN, 2 out of 6 LGN, metastatic lesions (n=5), abscesses (n=3) and PCNSL (n=2) showed contrast-enhancement. Non-facilitated diffusion was exhibited by 10 out of 14 HGN, 1 out of 6 LGN, 1 case of metastasis, all cases of lymphoma (n=2) and brain abscess (n=3). rCBV greater than 1.75 was seen in 11 of 14 HGN, 1 of 6 LGN, 1 of 3 brain abscess and all cases of PCNSL (n=2) & metastases (n=5). Cho/NAA greater than 2.2 from within the lesion was seen in 11 out of 14 HGN, 1 out of 6 LGN and all cases of PCNSL (n=2) and metastases (n=5). Cho/NAA greater than 1 from outside of the enhancing margin of the lesion was seen in 12 out of 14 HGN, 1 out of 6 LGN, 1 out of 5 metastases, 1 out of 3 brain abscess and none of the 2 cases of lymphoma (Table 2). Of the 9 inaccurately diagnosed cases, 1 case of primary CNS lymphoma was misdiagnosed as metastasis, 2 cases of HGN as brain abscess, 1 case of HGN as metastasis, 1 case of HGN as LGN, 1 case of LGN as HGN, 1 case of LGN as abscess / tumefactive demyelinating lesion (TDL), 1 case of brain abscess as HGN, and 1 case of metastasis (primary breast carcinoma) as HGN (Table 1).

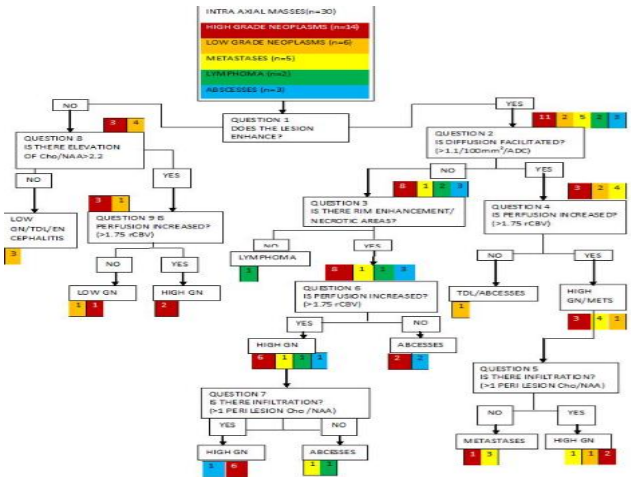

Table 1: Intra-axial brain masses with discordance on imaging and HPE.

HGN: Highgrade Neoplasm, **LGN**: Low grade Neoplasm, **TDL**: Tumefactive demyelinating lesion,**PCNSL**: Primary CNS lymphoma, **HPE**: Histopathological Examination. **NA**: Not applicable in the diagnostic algorithm.

HPE based diagnosis	Perfusion rCBV			Lesional SPS (Cho/NAA)			Perilesional SPS (Cho/NAA)			Diffusion : (100/mm^2/ ADC)		
	Raised (>1.75)	Not Raised (≤1.75)	NA	Raised (>2.2)	Not raised (≤2.2)	NA	>1	<1	NA	Facilitated (> 1.1)	Not facilitated (≤ 1.1)	NA
HGN (14)	11	3	0	11	3	0	12	2	0	4	10	0
LGN (6)	1	5	0	1	5	0	1	5	0	5	1	0
PCNSL (2)	2	0	0	2	0	0	0	2	0	0	2	0
Metastasis (5)	5	0	0	5	0	0	1	4	0	4	1	0
Brain abscess (3)	1	2	0	0	3	0	1	0	2	0	3	0

Table 2: Table showing imaging features in histopathologically different neoplasms.GN: High grade Neoplasm, LGN: Low grade Neoplasm, TDL: Tumefactive demyelinating lesion,PCNSL: primary CNS lymphoma, HPE: Histopathological Examination. SPS: Spectroscopy.

Fig 2 illustrates a case of imaging-based diagnosis of HGN and concordant histopathology.

S.No	rCBV	Lesion Cho/NAA	Perilesional Cho/NAA	ADC (100/mm^2/ ADC)	Nonenhancing areas(within enhancing lesion	Algorithm based diagnosis	HPE
1	1.64	2.10	NA	1.0	Yes	Abscess/TDL	HGN
2	1.58	1.92	NA	0.9	Yes	Abscess/TDL	HGN
3	1.90	0.70	>1	0.9	Yes	HGN	Abscess
4	3.25	1.40	<1	1.6	Yes	Metastases	HGN
5	1.86	1.90	>1	1.6	Yes	HGN	LGN
6	1.70	2.32	NA	1.5	Non enhancing lesion	LGN	HGN
7	0.86	1.91	NA	1.0	Yes	Abscess / TDL	LGN
8	2.9	7.1	>1	1.7	Yes	HGN	Metastases
9	2.3	NA	<1	0.6	Yes	Metastases	PCNSL

Fig 2 shows a well-defined intra-axial mass lesion involving right superior frontal and cingulate gyrus, with perilesional edema (A), non-facilitated diffusion (B & C, ADC value :0.8 x 10-3 mm2 /sec), lesional Cho/NAA: 15 (D), perilesional Cho/NAA: >1 (not shown in figure), rCBV : 9.1 (E) and the DSC mean curve revealing rapid steep fall in signal intensity (F).The algorithm based diagnosis and histopathology were concordant with diagnosis of HGN.

One case of primary CNS lymphoma (Fig 3) centred in the splenium of corpus callosum misdiagnosed as metastasis based on the diagnostic algorithm, showed restriction of diffusion (ADC value of 0.6), rCBV of 1.8, Cho/NAA < 1 outside of the enhancing margins, and presence of non-enhancing areas within the lesion.

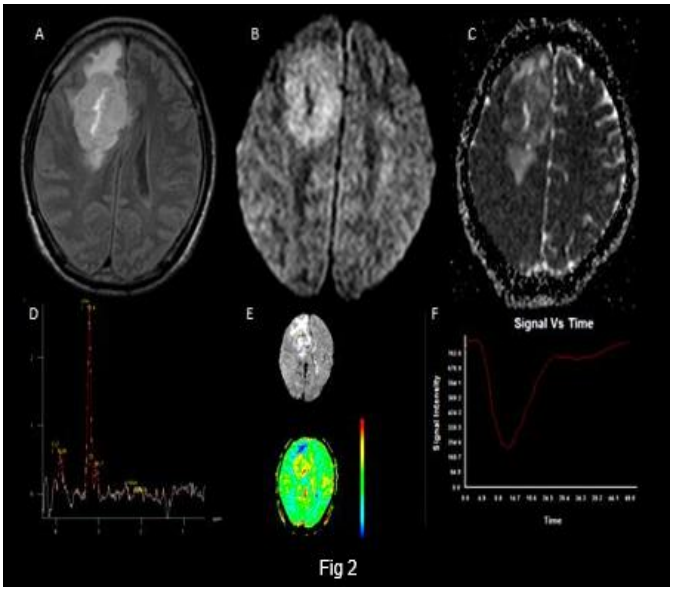

Fig 2

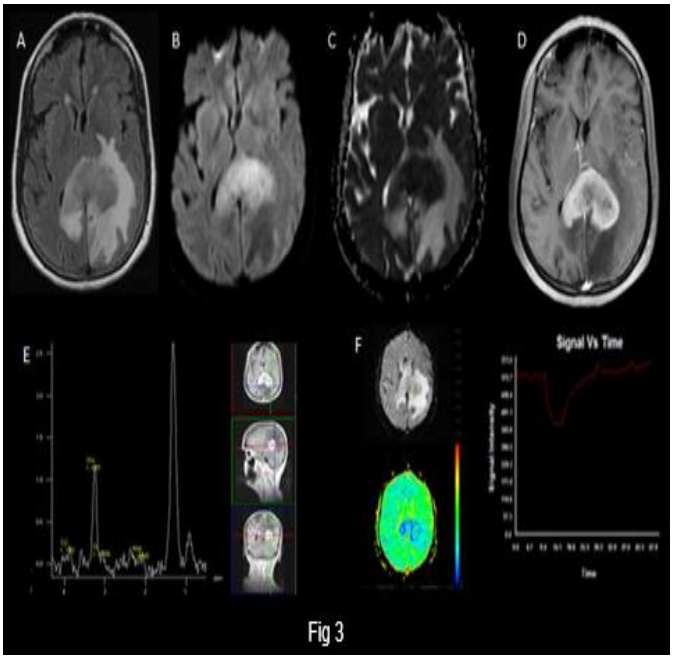

Fig 3

The sensitivity, specificity, positive predictive value (PPV) and negative predictive value (NPV) in differentiating neoplastic from non-neoplastic, HGN from LGN, HGN from metastases are detailed in Tables 3 and 4.

Discrimination	Accuracy	Sensitivity	Specificity	PPV	NPV
Neoplastic from non-neoplastic lesions	87	89 (70,97)	67 (13,98)	96 (77,100)	40 (7,83)
HGN versus LGN	88	91 (57,100)	80 (30,99)	91 (57,100)	80 (30,99)
HGN versus metastases	87	91 (57,100)	75 (22,99)	91 (57,100)	75 (22,99)

Table 3. Measures of accuracy of MRI based strategy in discriminating intra-axial brain lesions. HGN: High grade Neoplasm, **LGN**: Low grade Neoplasm, **NPV** = negative predictive value, **PPV** = positive predictive value (Data are percentages with 95% confidence intervals in brackets).

Discrimination	Accuracy	Sensitivity	Specificity	PPV	NPV
HGN versus LGN based on rCBV	80	79 (49,94)	83 (37,100)	92 (60,100)	63 (26,90)
HGN versus LGN based on lesional Cho/NAA	80	79 (49,94)	83 (37,100)	92 (60,100)	63 (26,90)
HGN versus metastases based on perilesional Cho/NAA ratio	82	83 (51,97)	80 (30,99)	91 (57,100)	67 (24,94)
HGN versus metastases based on lesional ADC	74	71 (42,90)	80 (30,99)	91 (57,100)	50 (17,83)

Table 4. Measures of accuracy of MRI based strategy in discriminating malignant brain

Lessions. HGN: High grade Neoplasm, **LGN**: Low grade Neoplasm, **NPV** = negative predictive value, **PPV** = positive predictive value (Data are percentages with 95% confidence intervals in brackets)

Discussion:

The characterization of tumour grade, more importantly differentiating low grade (WHO I-II) & high grade (WHO III-IV) gliomas, is crucial for decision-making in treatment. The conventional MRI appearances in enhancing malignant brain tumours (HGN, PCNSL and metastases) may be similar and not indicate a specific diagnosis. Advanced MR imaging plays a crucial role in non-invasive assessment of intra-axial brain masses and aid in making treatment decisions[2].

Contrast-enhancement is usually directly related to the progressively increasing grade of tumour (almost all GBMs show enhancement), and presence of enhancement in grade II tumours being associated with poorer outcome[3, 4, 5]. The glioma in the elderly may show subtle or no enhancement, despite being of high grade[6]. The heterogeneity of high grade tumours demands that biopsy be targeted from higher perfusion areas, rather than from the most enhancing region of the tumour to avoid sampling error and undergrading of tumour[7, 8]. DSC perfusion measures T2/T2* signal intensity in the brain tissue and the rCBV parameter obtained plays a key role in differential diagnosis of intra-axial brain masses[9, 10]. Lesions with high rCBV distinguishes tumour from non-tumour, corresponds to higher tumour grade, worse prognosis, increased microvessel density and directs biopsy sites with an increased likelihood of obtaining the highest-grade portion of tumour[10, 11]. Studies have consistently documented significantly lower rCBV in infectious lesions compared to metastases or high grade glioma[12, 13, 14]. Floriano VH *et al* concluded that rCBV cut-off value of 1.3 differentiated infectious from neoplastic lesions with sensitivity, specificity and accuracy of 97.8%, 92.6 % and 95% respectively[12]. Despite the usually higher rCBV in neoplasms, the potential for overlap does exist between non-neoplastic lesions and low-grade tumours[15]. No universally agreeable rCBV threshold exists to differentiate HGN from LGN[1, 16, 17, 18] with Ji HS *et al*[16], Nail Bulakbasi *et al*[17], Law M *et al*[18] and Al-Okaili RN *et al*[1] suggesting rCBV cut-off values of 2.93, 2.60, 1.75 and 1.75, respectively. Gliomas with high rCBV, specifically more than 1.75 progress faster and are associated with a poor prognosis[18]. Due to extravascular leakage of contrast and differences in post-processing software used, the measured rCBV value may not be generalised to all studies[19]. The combination of preload and post-processing correction can significantly improve the accuracy of rCBV values compared to preload method alone[20]. The glioblastoma can be differentiated from PCNSL using corrected CBV (CBV with contrast leakage correction) more accurately than using conventional (uncorrected) CBV parameter[21].

MRS plays an important role in differentiating intra-axial brain masses by assessing the internal milieu of metabolites. In our study, 11 out of the 14 cases of HGN showed Cho/NAA ratio more than 2.2. Studies by Law M *et al*[22] and Calvar JA *et al*[23] have also shown similar results. All cases of brain abscess (n= 3) in this study revealed reduced Cho/NAA ratio with similar results documented by Burtscher IM *et al*[24]and Kumar A *et al*[25]. Presence of high rCBV and Cho/Cr outside the enhancing portion of a tumour suggests primary high grade neoplasm and helps differentiate it from metastases. In our study, 12 of the 14 cases of HGN and only 1 case of metastasis (out of 5), revealed perilesional Cho/NAA ratio of >1. Similar results have been documented by Burtscher IM *et al*[24] and Law M *et al*[26]. MRS pitfalls include inaccurate assessment of small lesions (due to lower spatial resolution), requirement of trained personnel to accurately put regions of interest (excluding areas of calcification, hemorrhage and scalp fat) and different acquisition sequences and processing techniques.

MR-DWI by assessing cellularity of intra-axial brain masses is a useful tool to discriminate HGN and LGN. The ADC values show progressive reduction with higher tumour grade[27]. Statistically significant difference is noted in ADC values between lymphoma and grade III-IV glioma; however the there is no significant difference between glioblastoma multiforme, anaplastic astrocytoma and metastasis[28]. Documenting significant restriction of diffusion (due to presence of high cellularity and viscosity) on DWI helps differentiate brain abscesses from necrotic or cystic tumours with a sensitivity of 96% [29, 30]. However, the rarely encountered overlap in diffusion restriction between brain abscess and HGN can be countered by perfusion MR to arrive at the correct diagnosis[14].

Thus a multiparametric approach combining ADC, rCBV and MRS metabolites ratio contributed to a more accurate diagnosis, compared to these modalities used alone[1, 22, 28].

Limitations to this study include small cohort size, non-inclusion of immunocompromised patients and overlap in the imaging technique cut-off values (in various disease entities). The absence of a cut-off percentage value of the non-enhancing component in an enhancing lesion to be considered as necrosis on contrast-enhanced MRI (CE MRI) resulted in a few diagnostic errors.

Conclusion:

Diagnosing intra-axial brain masses using a combination of advanced imaging techniques (MRS, MR perfusion and DWI) in intra-axial brain masses is fairly accurate and should be resorted to whenever feasible. Modification in advanced imaging parametric cut-off values, inclusion of immunocompromised patients, inclusion of cut-off values to assign a lesion as necrotic on CE MRI, large cohort size with accordingly modified diagnostic algorithm is suggested to further validate the results of this study.

References:

[1] Al-Okaili RN, Krejza J, Woo JH, Wolf RL, O'Rourke DM, Judy KD, *et al*. Intraaxial brain masses: MR imaging-based diagnostic strategy–initial experience. Radiology 2007; 243: 539-50.

[2] Wen PY, Macdonald DR, Reardon DA, Cloughesy TF, Sorensen AG, Galanis E, *et al*. Updated response assessment criteria for high-grade gliomas: response assessment in neuro-oncology working group. J Clin Oncol. 2010; 28: 1963-72.

[3] Pope WB, Sayre J, Perlina A, Villablanca JP, Mischel PS, Cloughesy TF, *et al.* MR imaging correlates of survival in patients with high-grade gliomas. AJNR Am J Neuroradiol 2005; 26: 2466-74.

[4] Schafer ML, Maurer MH, Synowitz M, Wüstefeld J, Marnitz T, Streitparth F, *et al.* Lowgrade (WHO II) and anaplastic (WHO III) gliomas: differences in morphology and MRI signal intensities. Eur Radiol 2013; 23:2846-53.

[5] Chaichana KL, McGirt MJ, Niranjan A, Olivi A, Burger PC, Quinones-Hinojosa A, *et al.* Prognostic significance of contrast-enhancing low-grade gliomas in adults and a review of the literature. Neurol Res 2009; 31:931-9.

[6] Barker FG , Chang SM, Huhn SL, Davis RL, Gutin PH, McDermott MW, *et al*. Age and the risk of anaplasia in magnetic resonance non-enhancing supratentorial cerebral tumors. Cancer 1997; 80:936-41.

[7] Maia AC, Malheiros SM, da Rocha AJ, Stávale JN, Guimarães IF, Borges LR, *et al*. Stereotactic biopsy guidance in adults with supratentorial nonenhancing gliomas: role of perfusion-weighted magnetic resonance imaging. J Neurosurg 2004; 101:970-6.

[8] Lefranc M, Monet P, Desenclos C, Peltier J, Fichten A, Toussaint P, *et al.* Perfusion MRI as a neurosurgical tool for improved targeting in stereotactic tumor biopsies. Stereotact Funct Neurosurg 2012; 90:240-7.

[9] Rosen BR , Belliveau JW, Buchbinder BR, McKinstry RC, Porkka LM, Kennedy DN, *et al.* Contrast agents and cerebral hemodynamics. Magn Reson Med 1991; 19:285-92.

[10] Boxerman JL, Shiroishi MS, Ellingson BM, Pope WB. Dynamic susceptibility contrast MR imaging in glioma: review of current clinical practice. Magn Reson Imaging Clin N Am 2016; 24: 649-70.

[11] Sadeghi N, D'Haene N, Decaestecker C, Levivier M, Metens T, Maris C, *et al.* Apparent diffusion coefficient and cerebral blood volume in brain gliomas: relation to tumor cell density and tumor microvessel density based on stereotactic biopsies. AJNR Am J Neuroradiol 2008; 29:476-82.

[12] Floriano VH, Torres US, Spotti AR, Ferraz-Filho JRL, Tognola WA. The Role of Dynamic Susceptibility Contrast-Enhanced Perfusion MR Imaging in Differentiating between Infectious and Neoplastic Focal Brain Lesions: Results from a Cohort of 100 Consecutive Patients. PLoS ONE 2013; 8: e81509.

[13] Hakyemez B, Erdogan C, Bolca N, Yildirim N, Gokalp G, Parlak M, *et al*. Evaluation of different cerebral mass lesions by perfusion weighted MR imaging. J Magn Reson Imaging 2006; 24:817-24.

[14] Toh CH, Wei KC, Chang CN, Ng SH, Wong HF, Lin CP. Differentiation of brain abscesses from glioblastomas and metastatic brain tumors: comparisons of diagnostic performance of dynamic susceptibility contrast enhanced perfusion MR imaging before and after mathematic contrast leakage correction. PLoS One 2014; 9:e109172.

[15] Hourani R, Brant LJ, Rizk T, Weingart JD, Barker PB, Horská A. Can proton MR spectroscopic and perfusion imaging differentiate between neoplastic and nonneoplastic brain lesions in adults? AJNR Am J Neuroradiol 2008; 29:366-72.

[16] Shin JH, Lee HK, Kwun BD, Kim JS, Kang W, Choi CG, et al. Using relative cerebral blood flow and volume to evaluate the histopathologic grade of cerebral gliomas: Preliminary results. AJR 2002; 179:783-9.

[17] Bulakbasi N, Kocaoglu M, Farzaliyev A, Tayfun C, Ucoz T, Somuncu I. Assessment of diagnostic accuracy of perfusion MR Imaging in primary and metastatic solitary malignant brain tumors. AJNR Am J Neuroradiol 2005; 26:2187-99.

[18] Law M, Yang S, Babb JS, Knopp EA, Golfinos JG, Zagzag D, *et al.* Comparison of cerebral blood volume and vascular permeability from dynamic susceptibility contrast-enhanced perfusion MR imaging with glioma grade. AJNR Am J Neuroradiol 2004; 25:746-55.

[19] Hu LS, Kelm Z, Korfiatis P, Dueck AC, Elrod C, Ellingson BM, *et al.* Impact of software modeling on the accuracy of perfusion MRI in glioma. AJNR Am J Neuroradiol. 2015; 36:2242-9.

[20] Boxerman JL, Prah DE, Paulson ES, Machan JT, Bedekar D, Schmainda KM, *et al.* The role of preload and leakage correction in gadolinium-based cerebral blood volume estimation determined by comparison with MION as a criterion standard. AJNR Am J Neuroradiol 2012; 33:1081-7.

[21] Toh CH, Wei KC, Chang CN, Ng SH, Wong HF. Differentiation of primary central nervous system lymphoma and glioblastomas: comparisons of diagnostic performance of dynamic susceptibility contrast-enhanced perfusion MR imaging without and with contrast-leakage correction. AJNR Am J Neuroradiol 2013; 34:1145-9.

[22] Law M, Yang S, Wang H, Babb JS, Johnson G, Cha S, *et al.* Glioma grading: Sensitivity, specificity, and predictive values of perfusion Magnetic Resonance Imaging and Proton Magnetic Resonance Spectroscopic imaging compared with conventional Magnetic Resonance Imaging. AJNR Am J Neuroradiol 2003; 24:1989-98.

[23] Calvar JA, Meli FJ, Romero C, Calcagno ML, Yánez P, Martinez AR, et al. Characterization of brain tumors by MRS, DWI and Ki-67 labeling index. J Neurooncol 2005; 72:273-80.

[24] Burtscher IM, Skagerberg G, Geijer B, Englund E, Ståhlberg F, Holtås S. Proton MR Spectroscopy and Preoperative Diagnostic Accuracy: An Evaluation of

Intracranial Mass Lesions Characterized by Stereotactic Biopsy Findings. AJNR Am J Neuroradiol 2000; 21:84-93.

[25] Kumar A, Kaushik S, Tripathi RP, Kaur P, Khushu S. Role of in vivo Proton MagneticResonance Spectroscopy in the evaluation of adult brain lesions: Our preliminaryexperience. Neurol India 2003 Oct; 51: 474-8.

[26] Law M, Cha S, Knopp EA, Johnson G, Arnett J, Litt AW. High-grade gliomas and solitary metastases: differentiation by using perfusion and proton spectroscopic MR imaging. Radiology 2002; 222:715-721.

[27] Murakami R, Hirai T, Sugahara T, Fukuoka H, Toya R, Nishimura S, *et al.* Grading astrocytic tumors by using apparent diffusion coefficient parameters: superiority of a one- versus two parameter pilot method. Radiology 2009; 251:838-45.

[28] Cem Calli C, Kitis O, Yunten N, Yurtseven T, Islekel S, Akalin T. Perfusion and diffusion MR imaging in enhancing malignant cerebral tumors. Eur J Radiol 2006; 58:394-403.

[29] Chang SC, Lai PH, Chen WL, Weng HH, Ho JT, Wang JS, *et al*. Diffusion-weighted MRI features of brain abscess and cystic or necrotic brain tumors: comparison with conventional MRI. Clin Imaging 2002; 26:227-36.

[30] Reddy JS, Mishra AM, Behari S, Husain M, Gupta V, Rastogi M, *et al*. The role of diffusion-weighted imaging in the differential diagnosis of intracranial cystic mass lesions: a report of 147 lesions. Surg Neurol 2006; 66:246-50.